Published in final edited form as:
Atmos Pollut Res. 2017 March ; 8(2): 275–284. doi:10.1016/j.apr.2016.09.005.

A Reduced Form Model for Ozone Based on Two Decades of CMAQ Simulations for the Continental United States

P. Steven Porter[1,*], **S.T. Rao**[2], **Christian Hogrefe**[3], and **Rohit Mathur**[3]

[1]Porter-Gego, Idaho Falls, ID

[2]North Carolina State University, Raleigh, NC 27695

[3]AMAD/NERL, U.S.E.P.A., Research Triangle Park, NC, USA

Abstract

A Reduced Form Model (RFM) is a mathematical relationship between the inputs and outputs of an air quality model, permitting estimation of additional modeling without costly new regional-scale simulations. A 21-year Community Multiscale Air Quality (CMAQ) simulation for the continental United States provided the basis for the RFM developed in this study. Predictors included the principal component scores (PCS) of emissions and meteorological variables, while the predictand was the monthly mean of daily maximum 8-hour CMAQ ozone for the ozone season at each model grid. The PCS form an orthogonal basis for RFM inputs. A few PCS incorporate most of the variability of emissions and meteorology, thereby reducing the dimensionality of the source-receptor problem. Stochastic kriging was used to estimate the model.

The RFM was used to separate the effects of emissions and meteorology on ozone concentrations. by running the RFM with emissions constant (ozone dependent on meteorology), or constant meteorology (ozone dependent on emissions). Years with ozone-conducive meteorology were identified, and meteorological variables best explaining meteorology-dependent ozone were identified. Meteorology accounted for 19% to 55% of ozone variability in the eastern US, and 39% to 92% in the western US. Temporal trends estimated for original CMAQ ozone data and emission-dependent ozone were mostly negative, but the confidence intervals for emission-dependent ozone are much narrower. Emission-driven changes in monthly mean ozone levels for the period 2000–2010 ranged from 6.4 to 10.9 ppb for the eastern US and from 1.4 to 2.5 ppb for the western US.

Keywords

reduced form model; ozone; emissions; meteorology; community multiscale air quality model

[*]Corresponding author: pporter@uidaho.edu, 308 Evergreen Drive, Idaho Falls, Idaho, USA, 83401.

1. INTRODUCTION

In this study, a Reduced Form Model (RFM) for the continental US (CONUS) was developed from a 21-year Community Multiscale Air Quality (CMAQ) model simulation. A RFM is a mathematical relationship between the inputs and outputs of an air quality model, permitting estimation of additional modeling scenarios without having to run costly new modeling simulations. CMAQ inputs used for the RFM included monthly mean emissions and meteorology, while the CMAQ outputs of interest are the monthly means of the daily maximum 8-hour summer season surface ozone (May-September). The RFM was fit by stochastic kriging (Ankenman, 2010) applied to the Principal Component Scores (PCS) of the emissions and meteorology. The PCS form an orthogonal basis for the RFM inputs (Eder et al., 1993; Bakshi, 1998). In addition, a few PCS incorporate most of the variability of monthly mean emissions and meteorology, thereby reducing the dimensionality of the problem.

The 21-year CMAQ model run was created for a variety of purposes that did not initially include RFM development. Therefore, creation of the meteorological fields and emission inventories did not represent extra effort. In addition, the NOx and VOC emissions for some sources (e.g., mobile emissions) are correlated to a degree because they tend to occur together. Ozone simulations dedicated to RFM development, on the other hand, are typically designed to capture the ozone response to a range of emissions for a fixed set of meteorological conditions. For example, the RFM described in USEPA (2006) and compared to another reduced-form modeling approach in Foley et al. (2014) was based on 155 one-month model runs with emissions selected via statistical sampling of a wide range of emissions. In this USEPA RFM, the emissions are orthogonal and the meteorology is fixed.

During the CMAQ simulation period (1990–2010), monthly mean ozone values declined significantly in much of the eastern US and did not significantly change in much of the western US. At the same time, anthropogenic VOC and NOx emissions declined by roughly 50%. There were also significant changes in the prevailing meteorologican conditions during these 21 years.

The focus of our study is determining the inherent relationsships among emissions, meteorogy, and ozone embedded in the CMAQ model output spanning 21-years during which there have been substantial changes in the prevailing meteorology and emissions loading, and not on extreme ozone values stemming from wildfires or unusual meteorological conditions. There have been other studies that examined how well models can simulate peak ozone levels especially when estimates of emissions loading from wildfires are highly uncertain (Porter et al., 2015; Pavlovic et al. 2016).

Because results from the coupled meteorology-chemical transport (WRF-CMAQ) model are used in this study together with substantial changes in meteorology, emissions, and associated atmospheric chemistry, this RFM can serve as a first order approximation to detailed air pollution modeling. Never-the-less, the value of the results is limited to the range of meteorological and emissions conditions used in the model simulations.

2. Methods

2.1 Photochemical model set-up

This analysis relies on a photochemical model simulation, including emissions and meteorological inputs and the output ozone. A separate analysis was carried out that compares CMAQ ozone with ozone measured at monitoring sites (Xing etal, 2015). All references to ozone in this paper are to ozone estimated with CMAQ or the RFM.

Photochemical model simulations were performed for the years 1990–2010 with the in-line coupled Weather Research and Forecasting (WRF) - CMAQ version 5.0 modeling system (Wong et al, 2012). The modeling domain covered the CONUS at horizontal grid spacing 36 km and with 35 vertical layers between the surface and 100 mb. The simulations employed four-dimensional data assimilation (FDDA), for temperature, winds, and moisture above the planetary boundary layer using NCEP North American Regional Reanalysis (NARR) fields (~32 km horizontal resolution and 3-hourly temporal resolution) and upper air observations using the procedures suggested by Gilliam et al., (2012). In addition, soil moisture and temperature were indirectly nudged using surface observations. Details on the strengths of the nudging coefficients can be found in Gan et al. (2015).

Lateral chemical boundary conditions for the 36 km domain were prepared from a WRF-CMAQ simulation performed for the northern hemisphere for the same time period. These hemispheric simulations used a horizontal grid spacing of 108 km and 44 vertical layers of variable thickness between the surface and 50 mb. Emissions for the hemispheric simulations were based on the Emission Database for Global Atmospheric Research, version 4.2 (EDGARv4.2) (European Commission, 2011) and the Global Emission Inventory Activity (GEIS) database (Guenther et al., 1995). Additional details on these hemispheric simulations are provided in Xing et al. (2015). The use of hemispheric CMAQ together with continental CMAQ enabled specification of consistent boundary conditions for modeling simulations over CONUS.

The emissions for the 36 km CONUS simulations incorporated information from the US EPA National Emissions Inventory (NEI) for the years 1990, 1995, 1996, 1999, 2001, 2002 and 2005 as well as information on trends of activity data and emission controls over the entire period. A detailed description of the development of the emissions dataset is provided in Xing et al. (2013). Biogenic emissions were estimated in-line during the WRF-CMAQ simulation using BEIS, taking into account the effects of simulated meteorology on biogenic emissions. The wildfire emissions used in this study were based on the approach described in Xing et al. (2013). Specifically, the Xing et al. (2013) emission inventory used in this study relied on historical year-specific information about acres burned from the National Interagency Fire Center (NIFC, 2016) to adjust a climatological fire inventory for a given year. A comparison of WRF-CMAQ simulated trends in radiation, aerosol optical depth, and particulate matter trends against observations has been presented by Gan et al. (2015). In this approach, there was no explicit correlation between the simulated meteorology and the wildfire emission inventory, though in reality these emissions are modulated by meteorology in a complex way. Therefore, biogenic emissions were grouped with meteorology when considering changes in ozone.

For analysis purposes, the 36 km model domain was divided into eight (8) sub-regions (Figure 1) which were fit to separate RFMs. The sub-regions considered include Northeast (NE), Middle Atlantic (MA), Midwest (MW), South (S), West (W), Northwest (NW), West Coast (WC), and Southwest (SW).

The predicted variables were monthly means of the daily maximum 8-hour ozone concentrations at each model cell for the ozone season, defined as 1 May to 30 September (153 days or 5 months). Predictors included monthly means of emission and meteorological variables. Table 1 lists the emission sources while meteorological variables are shown in Table 2.

The emission sources are defined as follows (USEPA, 2016; TCEQ, 2016). Area sources are **s**tationary sites and processes that do not meet the reporting requirements for point sources. Examples include stationary source fuel combustion, small surface coating operations, feedlots, crop burning and forest fires. Non-EGU point sources are stationary and meet a given states reporting requirements. EGU refers to Electricity Generating Unit'. Since about 2000, EGU point sources have been measuring and reporting emissions. Hourly measured NOx values were used in the CMAQ simulations. On-road mobile emission sources include motor vehicles traveling on public roadways. The emissions are either combustion-related or evaporated fuel. Non-road mobile sources do not usually operate on roads. They include equipment used in agriculture, lawns, aircraft, commercial marine vessels (CMV) and drilling rigs. Examples of biogenic sources include crops, trees and soil.

2.2 RFM Development

The RFMs are a fit of CMAQ ozone to the Principal Components Scores (PCS) of the predictor variables (emissions and meteorology rescaled to 0 mean and unit variance) using Stochastic Kriging (SK) (Ankenman, 2010). The PCS form an orthogonal basis for the predictors (X) with scores (XS):

$$XS = (X - \bar{X}) * XW\,,\; X = XS * XW' + \bar{X} \quad (1)$$

Scores are the orthogonal representation of X in the principal component space, while loadings (XW) are the coefficients (weights applied to X) that accomplish the transformation between X and XS.

The initial emissions+meteorology dimension of a given region equals the product of the number of emission and meteorological variables (22) and the number of model cells (between 298 and 1637, depending on region). Dimension reduction was accomplished when a few 'scores' (PCS) explaining much of the variability in X was retained (see Eder et al, 1993 for other air quality applications of principal component analysis). In this case, the set of PCS explaining more than 95% of the predictor variability was retained (ranging between 14 to 28 PCS depending on region). Since a separate RFM was developed for each region, the resulting RFMs do not account for the effects of emission changes in one region on air quality in a different region.

SK is a geostatistical method for which emissions and/or meteorology have the role of location coordinates. Ozone values coincident with a particular set of PCS (derived from emissions and meteorology) are interpolated from nearby ozone values (Ankenman et al, 2010). An interpolation estimate looks like:

$$\hat{Y} = \mu + B_1 Y_1 + B_2 Y_2 + B_3 Y_3 + B_4 Y_4 + B_5 Y_5 \ . \ . \ . + B_n Y_n + \varepsilon_i \quad (2)$$

The Y_i are neighbors of an ozone value at a location of interest ($\widehat{Y}$) in the sense that they are close to $\widehat{Y}$ in terms of the PCS of emissions and meteorology. The B_i's are constants derived from the correlation between different ozone values as a function of their distance apart (as noted, distance in terms of the PCS of emissions and/or meteorology). While equation (2) is linear, SK ozone response is nonlinear with respect to emissions and meteorology (unlike projection onto latent structures, which is a linear model based on PCS (Wold et al, 2001)).

While the PCS are indeed orthogonal, highly collinear variables are separated in an arbitrary fashion. For example, monthly mobile source VOC and NO_X are highly correlated in every sub-domain (average $R^2 > 0.95$). Therefore, for most of the RFM applications that follow, the effects of NO_X and VOC on ozone are considered jointly. 'Joint' treatment in this context means that VOC's and NOX for a given source were set to the same year. They did not take on equal values or change from year-to-year by equal amounts. A cross-validation analysis of this RFM can be found in Porter (2016).

2.3 RFM application

After SK estimation with the 21-year set of predictor and output variables, the RFM was run with either meteorology or emissions fixed. To determine the ozone response to emissions, for example, the model was driven with meteorology from a particular year (2010) while emissions were allowed to vary. Conversely, the ozone response to meteorology was determined from a RFM run with a single year of emissions (also 2010) and meteorology varying. While mean ozone values depend on the choice of the year used for meteorology or emissions, year-to-year ozone responses are nearly independent of the choice of year.

Because this RFM was developed from a multi-decadal modeling simulations covering a wide range of meteorological and emission conditions, it enables us to rapidly assess the impacts of various emission control scenarios envisioned for different weather conditions to arrive at an emission control strategy that could be a potential candidate for attainment demonstration, after which detailed WRF-CMAQ type modeling would be conducted for developing emission control strategies needed to attain the standard as part of the SIP.

2.4 Confidence intervals for the metrics of interest

RFM metrics of interest included region-wide mean values of temporal trends, ozone ranges over the 21–year modeling time span, and the ozone response to changes in emissions. Confidence intervals (95%) for metrics were calculated from bootstrap resamples (Efron and Tibshirani, 1993) in each region. For a given metric, 200 bootstrap resamples were taken for

all model cells. A 95% confidence interval was defined as the 2.5^{th} and 97.5^{th} percentiles of the 200 bootstrap resamples.

3. RESULTS AND DISCUSSION

3.1 CMAQ-simulated ozone

CMAQ monthly mean ozone concentrations for July 1990 and 2010 and their difference (1990 minus 2010) are presented in Figure 2. It is evident that changes in ozone during the modeling time span were largest in the eastern half of the US. Much of the western US has a positive change. Temporal trends (linear regression with time) for the CMAQ sub-domains are provided in Table 3 (Row 1), which reveals the percent of each region with significant positive and negative trends. For the eastern US (NE, MA, MW, S), the percentage of model cells with significant negative trends ranges from 35% to 87%. None of the cells in these regions have significant positive trends. For each of the western US sub-domains (W, NW, WC, SW), there are 5% or fewer cells with significant negative trends. This pattern of trends is consistent with those seen in ozone observations (Porter, 2016).

3.2 Emissions

While VOC emission inventories fell in much of the domain over the time span of the model run (Table 3, Rows 2–13), increases occurred with non-road VOC (VNR) in all regions and area source NO_X (NAR) in MW, S, W, and WC. Biogenic VOC (VBI) and NO_X (NBI) emissions increased in the W and WC regions.

3.3 Meteorology

The CMAQ meteorological variables typically are trend-free (Table 4). However, there are exceptions including temperature (T2) and solar radiation (R2), which have positive trends over much of the MW, W, NW and WC regions; these trends might be attributed to climate change and reduction in sulfate concentrations due to controls on SO_2 emissions. Relative humidity and soil moisture have negative trends for much of the W and NW regions.

Taken together, the emission and meteorological variables suggest that decreases in ozone in the eastern US are mostly due to decreasing VOC and NO_x emissions, while increases in ozone in the western US coincide with changes in meteorology (increases in temperature and solar radiation, and decreases in relative humidity and soil moisture), global pollution burden, and an increase in biogenic emissions. Jaffe and Ray (2007) speculate that summer season ozone increases in western states may be due, among other things, to increased biomass burning (note the positive trend for area VOC and NOx emissions in much of the west) and increasing ozone background levels due to increased emissions from Asia.

3.4 Ozone response to meteorology vs. emissions

The RFM was used to separate ozone responses to meteorology from those due to emissions. At a monthly time scale, the separation provides a smooth trending response to emissions (2010 meteorology) and a highly variable response to meteorology (Figure 3 for the NE region). When emissions are fixed (2010 values, red line), one would conclude that the year 1994 was conducive to ozone formation (maximum value for the red line), while the year

2000 was meteorologically the least ozone conducive year (minimum value for the red line). Good and bad ozone years from the meteorological standpoint for all regions are summarized in Table 5.

The emission-dependent components for all years are displayed in Figure 4. Meteorology was fixed at 2010 values. Four of the eight regions (NE, MA, MW and S) showed substantial reductions in ozone beginning about 2000. The timing of these reductions coincides with the phasing-in of NO_x controls on power plants in the Ozone Transport Region (OTR) in 1999 and the full implementation of NO_x controls on power plants in 22 states in the eastern U.S. under the NO_x SIP call by 2004. The other four regions show little change over the 21-year period. Slope estimates (linear regression against year, ppb/year) and confidence intervals for each region are given for three time periods (1990–2010, 1990, 2000, and 2000–2010) in Table 6. With respect to CMAQ ozone, there are significant negative slopes for the 1990–2010 period in the NE, MA, MW, and S regions, none significant for the 1990–2000 period, and significant negative slopes for the MA, MW, S and NW regions for the 2000–2010. For the 1990–2010 and 2000–2010 periods, all of the emission-dependent slopes are significant at the 1% or 5% level. For the 1990–2000 period, there are significant positive slopes for the MA, MW and S regions, with slopes in the other regions not significant at the 5% level. While some of the original CMAQ ozone slopes are also significant, the confidence intervals for the emission-dependent slopes are all much smaller, in some cases by a factor of 20.

Meteorologically- and emission-dependent ozone (using 2010 emissions and meteorology, respectively) were fit to the meteorological variables and emissions, respectively, using stepwise regression (Table 7). The first two rows of Table 7 are the variances in meteorologically and emission dependent ozone explained by meteorology and emissions, respectively. The variability in the original ozone time series explained by meteorology, emissions or both is displayed in rows three through five, respectively, of Table 7. In regions with pronounced downward temporal emission trends (NE, MA, MW, S), emissions explain 46% to 74% of ozone variability, while in the other four regions, the fraction explained by emissions ranges from 1% to 33%. The percent explained by emissions in the W region is due to a large increase in area source emissions occurring in 2006 and 2007, that was strongly tied to ozone during that time. We suspect wildfires to be the driving force for this increase in area source emissions. As mentioned above, the Xing et al. (2013) emission inventory used in this study relied on historical year-specific information about acres burned from the National Interagency Fire Center to adjust a climatological fire inventory for a given year. As shown in Figure 7h of Xing et al. (2013) and the table of acres burned (NIFC, 2016) 2006 and 2007 were indeed the years with the highest amount of acres burned and, consequently, the highest amount of wildfire emissions in the 1990 – 2010 emission inventory compiled by Xing et al. (2013).

Much of the variability of emission-dependent ozone is due to the temporal trend in emissions. To show the impact of emission trends, linear temporal trends were subtracted from CMAQ ozone, as well as emission- and meteorologically-dependent ozone. After detrending, ozone variance explained by emissions decreases while that explained by meteorology increases in those regions where there is a trend (Rows 7– 9 of Table 7). An exception occurs in the W region (again due to the spike in area sources that is not removed

by detrending). The other western U.S. regions are left almost unchanged by detrending (since they had little or no trend to begin with).

3.5 Temporal evolution of ozone response to emissions

The ozone response to emissions was assessed by plotting regionally-averaged emission-dependent ozone against scaled emissions (0–1 basis, Figure 5 for the NE region). The emission-dependent ozone values are shifted by subtracting the maximum ozone value (usually occurring near the beginning of the simulation period) so as to show ozone changes as emissions decline with time. The lower right panel, the response to changes in all emissions for the NE region, has a plateau on the right (corresponding to the first ten years of the simulation), a steep mid-portion, and a gradual reduction in slope in the lower left of the plot. The range in monthly mean ozone over the entire plot is about 8 ppb.

The other panels of Figure 5 reveal the ozone response to changes in individual sectors for the NE region. The mobile source plots for all regions have the clearest connection to emission-dependent ozone, having the most linear relationship of all sectors and all regions (not shown). Mobile source emissions trend smoothly downward during the simulation period due to steady fleet turnover. Reductions in other emission sources were not steadily downward. Decreases in EGU emissions, as noted above, began to appear about 1999.

Ranges in emission-dependent ozone with 95% confidence intervals for all regions and the years 2000–2010 are shown in Table 8. For some sources the confidence interval overlaps 0, especially in the western US where changes in ozone were small. Mobile source-dependent ozone ranged between 2.3 and 3.7 ppb for the eastern US and 0.1 to 1.0 ppb for the western US.

The response to EGU's is smaller than expected (0.4 to 0.8 ppb in the eastern US) perhaps because the regional RFM's do not account for the effects of emission changes in one region on air quality in a different region. It is also extremely difficult to accurately simulate ozone levels in complex urban environments even with high-resolution models, much less with 36km resolution as in this application. Emissions from mobile sources dominate in the early morning hours and plumes from EGUs are trapped aloft. As the boundary layer starts to grow, power plant plumes are entrained into lower levels and interact with locally-generated mobile, area, and other emissions to produce ozone and well mixed through the entire boundary layer.

The range of anthropogenic-dependent emissions for all model grid cells shows that the area for response greater than about 10 ppb is limited to the eastern half of the US (Figure 6, a spatial display of the information in Figure 5). For much of the western US, the range is close to 0.

3.6 Relationship between summer mean and annual 4th highest daily maximum 8-hr ozone concentrations

Finally, we consider the relationship between the regulatory design value (three-year running mean of the annual 4th highest daily maximum 8-hr ozone values) and the three-year running mean of the seasonal average derived from the monthly mean values used in this

study (plotted against each other in Figure 7). There is often a strong relationship between seasonal mean ozone and annual 4th highest values because a combination of the synoptic forcing and baseline concentration level (say, seasonal mean) dictates extreme ozone levels (Rao et al., 1996; Rao et al., 1997; Hogrefe et al, 2000; Rao et al, 2011). Therefore, understanding the behavior of the mean is important for trend assessments and for assessing the impact of emission controls on peak ozone levels. It is evident in Figure 7 that for several of the eight regions, the linear relationship is quite strong (R^2 greater than 0.9). For all eight regions, the p value for the relationship is less than 0.01.

4. Summary

A RFM was fit to the monthly mean values of daily maximum 8-hr ozone, emissions and meteorology of a CMAQ simulation for the CONUS for the years 1990–2010. The RFM was estimated from the principal component scores of emissions and meteorology using stochastic kriging. During this time ozone and emissions both declined in much of the eastern US. In the western US, CMAQ ozone was mostly unchanged even as emissions decreased.

Applications of the RFM included separating the effects of emissions and meteorology on changes in ozone concentration. Years with ozone-conducive meteorology were identified and ozone variability was attributed to emissions or meteorology. Temporal trends in emission-dependent ozone were estimated and compared with original (CMAQ) ozone. The emission-dependent ozone response of CMAQ to changing emissions was found to have changed over time.

Downward trends in emission-dependent monthly mean daily maximum 8-hour ozone (CMAQ estimated ozone) began in the eastern US about 2000 and ranged from −0.65±0.06 to −1.07±0.20 ppb/year, depending on region. This improvement is attributable to the implementation of NOx control programs in the OTR and OTAG regions. Trends in the western US ranged from −0.05±0.02 to −0.25±0.04 ppb/year. Trends estimated from CMAQ ozone were mostly negative but with much larger confidence intervals. Ozone trends in the western U.S. were significantly correlated with trends in biogenic VOCs and biogenic NOx, temperature and relative humidity.

Meteorology explains between 19% and 55% of ozone variance, and emissions 46% to 74% in the eastern US. Much of the ozone variability due to emissions was attributed to the downward trend in emissions. In the western US, meteorology was responsible for 39% to 92% of ozone variation.

Of all the individual sources considered in this study, the mobile sector has the clearest (most linear) connection to emission-dependent ozone as typified by Figure 5. However, as stated in Section II A, the RFM developed in this study does not account for the effects of emission changes in one region on air quality in a different region.

As noted above, because results from the WRF-CMAQ coupled model are used in this study together with substantial changes in meteorology and emissions, this metamodel can serve as a first order approximation to detailed air pollution modeling. In addition, the usefulness

of the results is limited to the range of meteorological and emissions conditions used in the model simulations.

Acknowledgements

Although this paper has been reviewed and approved for publication by the U.S. Environmental Protection Agency, it does not necessarily reflect the Agency's views or policies. One of the authors (P.S. Porter) acknowledges the support from the Coordinating Research Council under contract A-89.

V. References

Ankenman B, Nelson BL and Staum J. 2010 Stochastic Kriging For Simulation RFMing. Operations Research Vol. 58, No. 2, Mar-Apr, pp. 371–382

Bakshi B 1998 Multiscale PCA with application to MSPC monitoring, AIChE J. 44, pp. 1596–1610.

Eder BK, Davis JM and Bloomfield P. 1993 A characterization of the spatiotemporal variability of non-urban ozone concentrations over the eastern United States. Atmospheric Environment Part A General Topics 27(16):2645–2668, 10

Efron B and Tibshirani R, R. 1993 An Introduction to the Bootstrap. Chapman & Hall/CRC, Boca Raton, FL.

European Commission: Joint Research Centre (JRC)/Netherlands Environmental Assessment Agency (PBL). Emission Database for Global Atmospheric Research (EDGAR), release version 4.2., available at: http://edgar.jrc.ec.europa.eu, 2011.

Foley KM, Napelenok SL, Jang C, Phillips S Hubbell BJ, and Fulcher CM. 2014 Two reduced form air quality modeling techniques for rapidly calculating pollutant mitigation potential across many sources, locations and precursor emission types. Atmospheric Environment 98: 283–289

Gan C-M, Pleim J, Mathur R, Hogrefe C, Long CN, Xing J, Wong D, Gilliam R, and Wei C: Assessment of long-term WRF–CMAQ simulations for understanding direct aerosol effects on radiation "brightening" in the United States, Atmos. Chem. Phys, 15, 12193–12209, doi:10.5194/acp-15-12193-2015, 2015

Guenther A, Hewitt CN, Erickson D, Fall R, Geron C, Graedel T, Harley P, Klinger L, Lerdau M, McKay WA, Pierce T, Scholes B, Steinbrecher R, Tallamraju R, Taylor J, and Zimmerman P: A Global Model of Natural Volatile Organic Compound Emissions, J. Geophys. Res, 100, 8873–8892, 1995.

Hogrefe C; Rao ST; Zurbenko IG; Porter PS 2000 Interpreting the Information in Ozone Observations And Model Predictions Relevant to Regulatory Policies in the Eastern United States; Bull. Amer. Meteor. Soc; vol 81, pp 2083 – 2106.

Jaffe D and Ray J. 2007 Increase in surface ozone at rural sites in the western US. Atmospheric Environment 41: 5452–5463

National Interagency Fire Center. 2016 http://www.nifc.gov/fireInfo/fireInfo_stats_totalFires.html, accessed 2016.

Pavlovic R, Chen J, Anderson K,, Moran MD, Beaulieu P-A, Davignon D,,and Cousineau S. 2016 The FireWork air quality forecast system with near-real-time biomass burning emissions: Recent developments and evaluation of performance for the 2015 North American wildfire season. JAWMA 66: 819–841

Porter PS 2016 Ozone RFM for the Continental US: Model Inputs, Development and Performance. CRC Report No. A-89–2

Porter PS, Rao ST, Hogrefe C, Gego E and Mathur R. 2015 Methods for reducing biases and errors in regional photochemical model outputs for use in emission reduction and exposure assessments. Atmospheric Environment 112, pp 178–188,

Rao ST, Zurbenko IG and Porter PS. 1996 Dealing with the Ozone Non-Attainment Problem in the Eastern United States. Environmental Manager, vol 1, pp. 17–31

Rao ST, Zurbenko IG, Neagu R, Porter PS, Ku JU, and Henry RF. 1997 Space and time scales in ambient ozone data. Bull. American Meteorological Society, vol 78, pp. 2153–2166

Rao ST, Porter PS, Mobley D, and Hurley F. 2011 Understanding the Spatio-Temporal Variability in Air Pollution Concentration, Environmental Manager, 11, pp 42–48.

TCEQ (Texas Commission on Envrionmental Quality). 2016 http://tceq.state.tx.us/airquality/areasource/Sources_of_Air_Pollution.html/#Non-Road, accessed January 2016.

U.S. Environmental Protection Agency. 2016 https://www.epa.gov/air-emissions-inventories/national-emissions-inventory, accessed March

U.S. Environmental Protection Agency. 2006 Technical Support Document for the Proposed Mobile Source Air Toxics Rule: Ozone Modeling, Office of Air Quality Planning and Standards Research Triangle Park, NC

Wong DC, Pleim J, Mathur R, Binkowski F, Otte T, Gilliam R, Pouliot G Xiu A Young JO, and Kang D. 2012 Geosci. Model Dev, **2012**, 5, 299–312, doi:10.5194/gmd-5-299-2012.**2012**

Xing J, Mathur R, Pleim J, Hogrefe C, Gan C-M, Wong DC, Wei C, Gilliam R, and Pouliot G. 2015 Observations and modeling of air quality trends over 1990–2010 across the Northern Hemisphere: China, the United States and Europe Atmospheric Chemistry and Physics 15(5):2723–2747 · 3

Xing J; Pleim J; Mathur R; Pouliot G; Hogrefe C; Gan C-M; and Wei C 2013 Historical gaseous and primary aerosol emissions in the United States from 1990 to 2010 Atmos. Chem. Phys 13, 7531–7549, doi:10.5194/acp-13-7531-2013.

Xing J, Mathur R, Pleim J, Hogrefe C, Gan C-M, Wong DC, Wei C, Gilliam R, and Pouliot G: Observations and modeling of air quality trends over 1990–2010 across the Northern Hemisphere: China, the United States and Europe, Atmos. Chem. Phys, 15, 2723–2747, doi:10.5194/acp-15-2723-2015, 2015

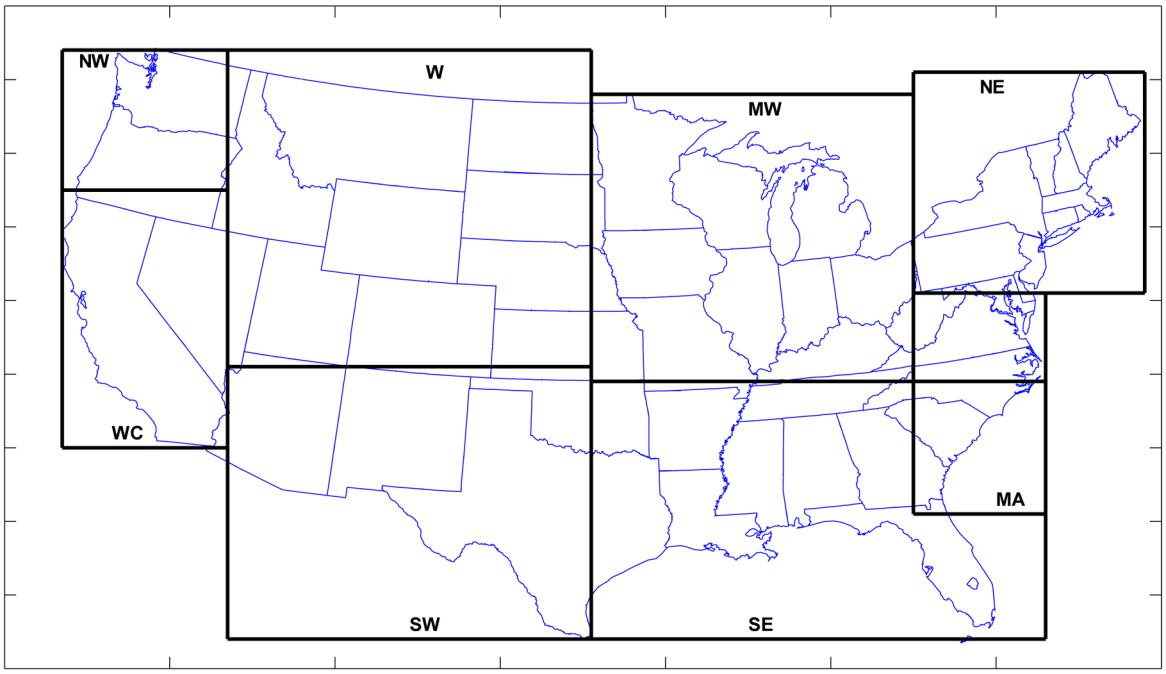

Figure 1.

Model domain divided into eight regions: Northeast (NE), Mid-Atlantic (MA), Midwest (MW), South (S), West (W), Southwest (SW), Northwest (NW), and West Coast (WC). The MA region overlaps parts of the S.

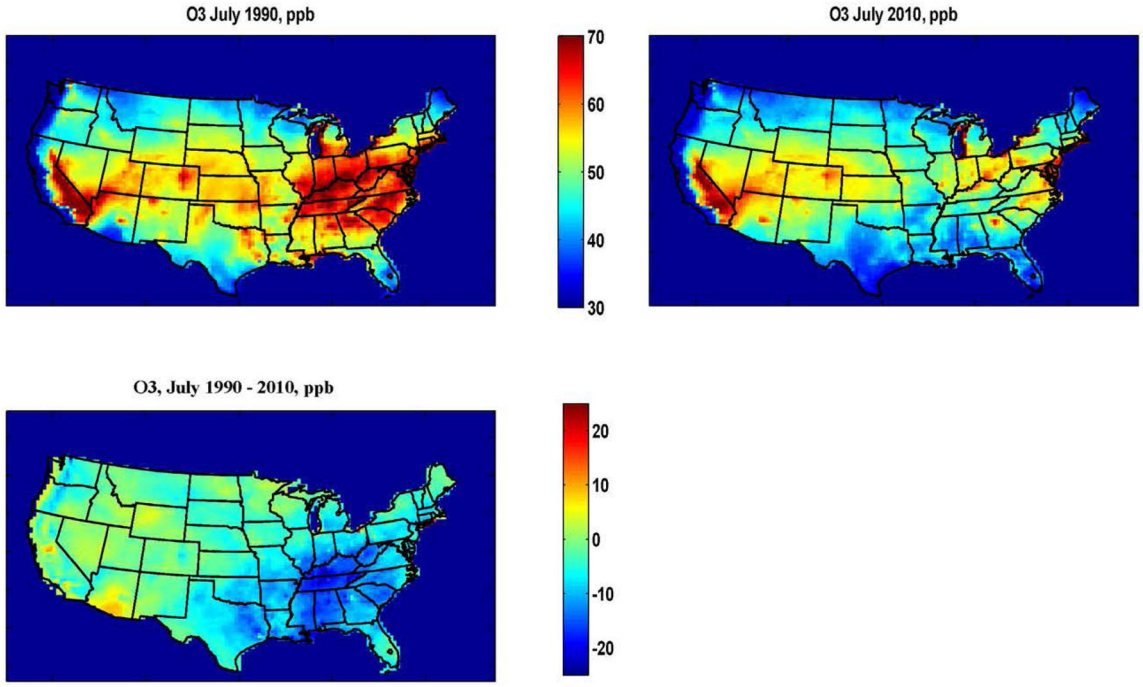

Figure 2.
Ozone: July 1990 (upper left), July 2010 (upper right), and their difference (lower left).

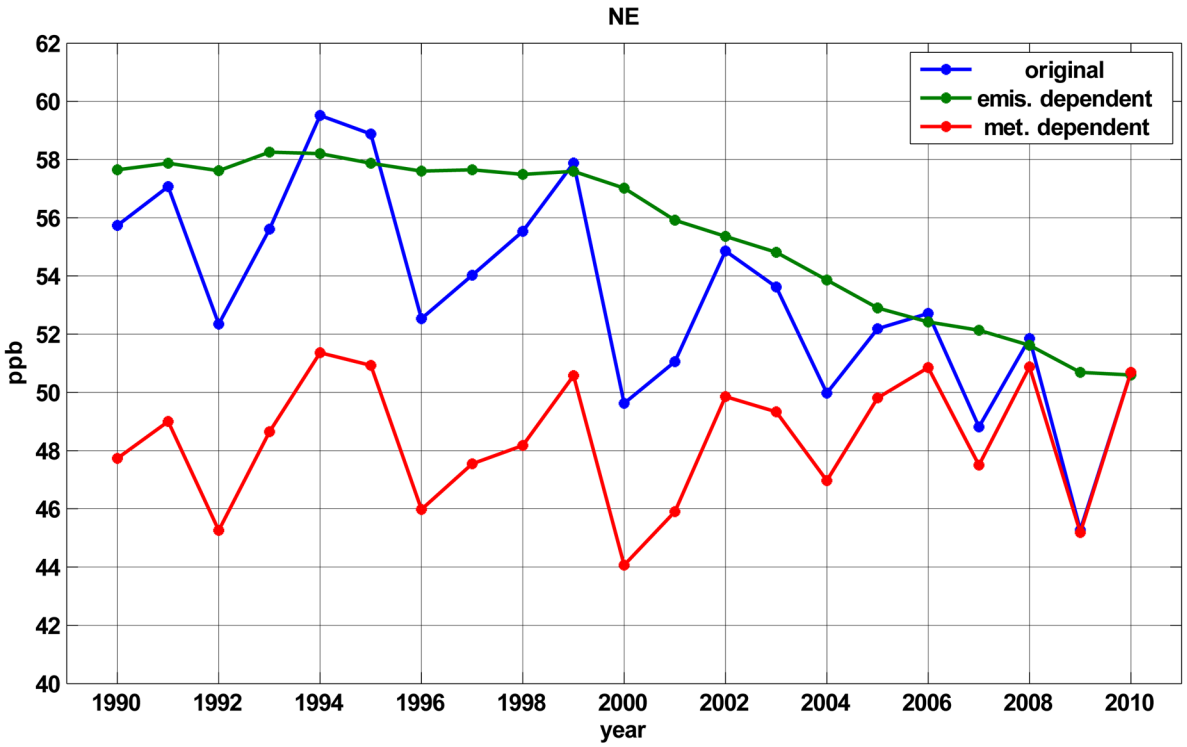

Figure 3.
CMAQ ozone (original, blue), emission-dependent ozone (green), and meteorologically-dependent ozone (red).

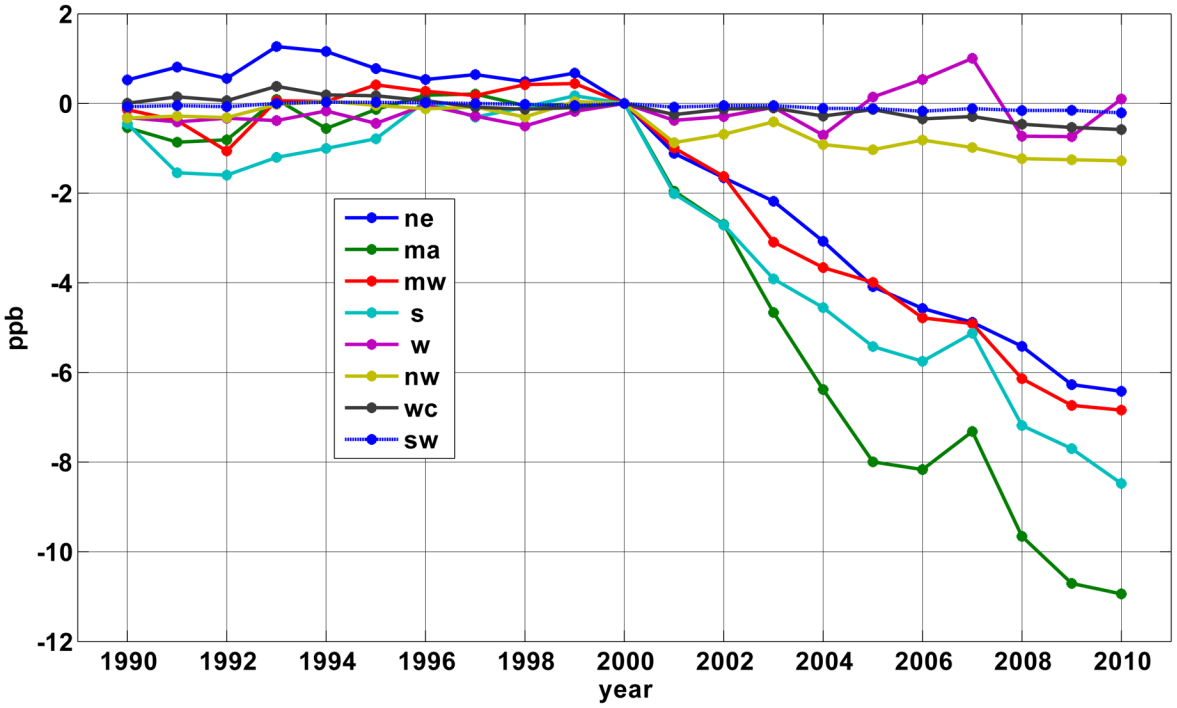

Figure 4.
Emission-dependent ozone: regional means for July.

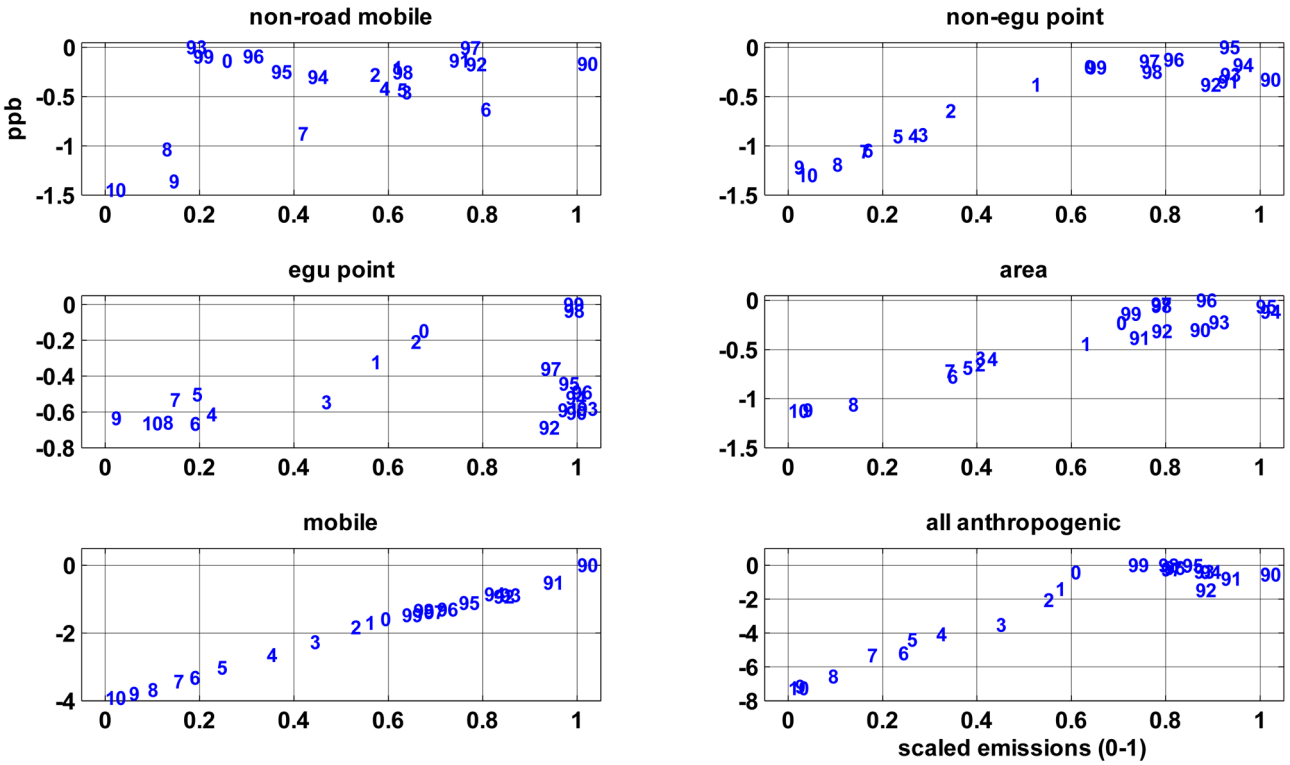

Figure 5.

NE region: Emission-dependent ozone (ppb) vs. combined NOx and VOC emissions (scaled from 0 to 1). Emission-dependent ozone the value obtained by subtracting the maximum ozone value. Symbols indicate year (‘10’ = 2010, ‘93’ = 1993)

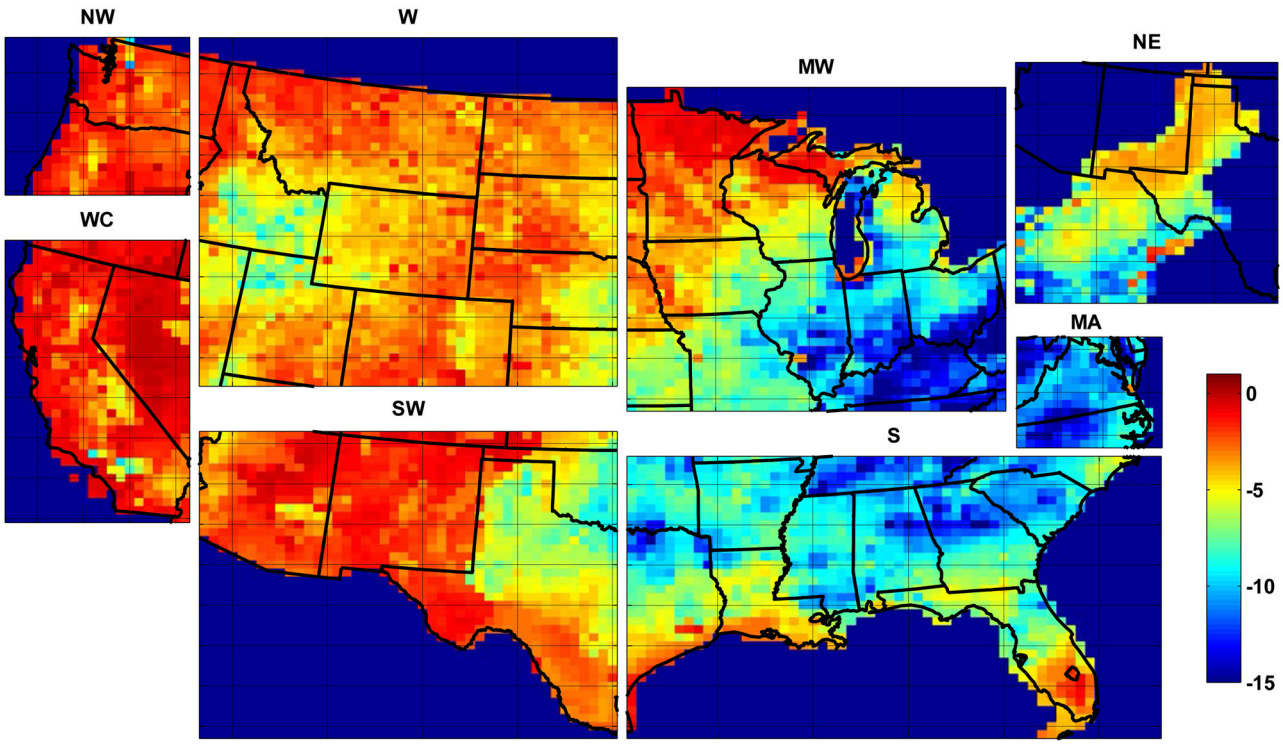

Figure 6.

Ozone response (ppb) to scaled anthropogenic emissions (0 – 1 scale), 2000–2010. This is a spatial version of Figure 5 for the period 2000–2010, showing the range of ozone values at each model cell.

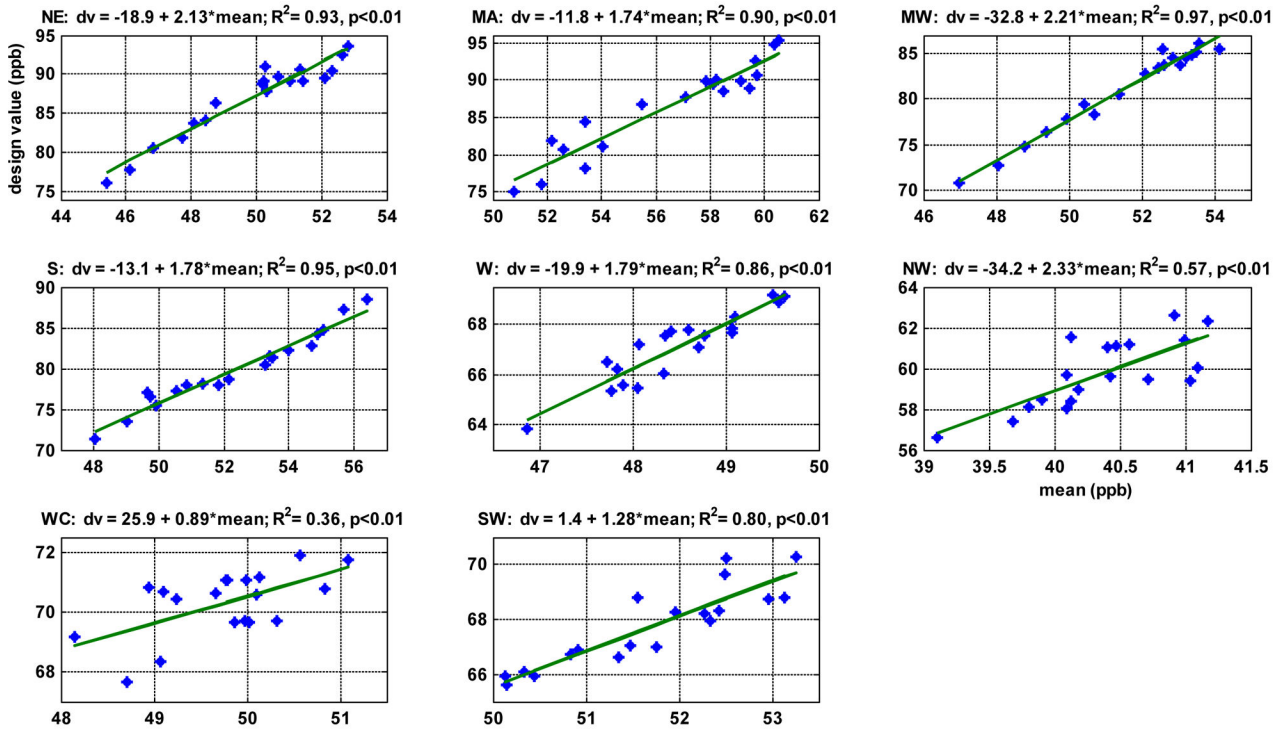

Figure 7.

Three year running mean of the annual 4th highest ozone values plotted against three-year running seasonal mean. The solid green line is the linear relationship between the two. The numbers above each panel are the linear relationship parameters (intercept, slope, R2, and slope p values).

Table 1.

Emissions. VOC acronyms preceded by ‘V’, and NOx emissions preceded by ‘N’.

emission source (VOC and NO_X)	acronyms	spatial scale
area	VAR, NAR	36 km
non-EGU point	VNE, NNE	
EGU point	VEG, NEG	time scale
on-road mobile	VMO, NMO	monthly mean
non-road mobile	VNR, NNR	
biogenic	VBI, NBI	

Table 2.

Meteorology

	acronyms	spatial scale
planetary boundary layer	PB	
pressure	P	36 km
temperature, 2m	T2	
solar radiation, 2m	R2	time scale
water vapor mixing ratio, 2m	Q2	monthly mean
relative humidity	RH	
precipitation	PR	
soil moisture	SM	
u wind	U	
v wind	V	

Table 3.

Temporal trends in ozone and emissions (1990 – 2010): percent of model grid cells in a given region with trends significant at the 95% level (see Table 1 for definitions of the emission acronyms).

region:	NE		MA		MW		S		W		NW		WC		SW	
emission	+	−	+	−	+	−	+	−	+	−	+	−	+	−	+	−
O3	0	56	0	87	0	35	0	35	4	0	11	3	5	0	2	2
VNR	30	3	71	0	29	19	46	3	22	4	40	0	23	2	53	2
VNE	5	83	2	86	6	84	7	79	24	55	19	50	10	73	20	69
VEG	18	40	40	2	26	14	46	9	27	25	67	22	39	7	47	13
VAR	0	97	0	96	3	95	0	83	2	24	0	38	15	27	10	33
VMO	0	100	0	100	0	100	0	100	0	100	0	100	0	100	0	98
VBI	1	0	0	0	17	0	1	0	76	0	0	3	47	0	19	0
NNR	0	84	0	89	1	91	0	91	2	88	0	91	2	86	2	88
NNE	8	67	9	60	13	52	12	65	36	34	15	40	5	53	25	58
NEG	7	73	12	47	14	49	16	40	19	35	25	25	0	67	15	44
NAR	26	50	33	42	48	26	45	24	39	1	20	11	39	15	57	1
NMO	0	100	0	99	0	100		96	0	100	0	100	0	99	3	97
NBI	2	0	0	11	5	2	4	3	45	1	0	3	38	0	19	0

+ uptrend, − downtrend

Blue: downtrends > 24%; red: uptrends > 24%

Table 4.

Temporal trends in meteorological variables (1990 – 2010): percent of model grid cells with trends significant at the 95% level (see Table 2 for definitions of the meteorological acronyms).

region:	NE		MA		MW		S		W		NW		WC		SW	
	+	−	+	−	+	−	+	−	+	−	+	−	+	−	+	−
PB	1	14	5	1	2	10	0	6	1	3	0	11	0	25	0	7
P	0	0	0	0	0	0	0	2	1	0	0	0	0	51	0	15
T2	2	0	0	0	26	0	2	0	83	0	9	6	53	0	20	0
R2	15	0	1	0	31	0	0	1	39	0	63	0	9	0	0	5
Q2	22	0	0	0	3	0	4	3	1	0	0	0	0	0	7	0
PR	27	0	0	9	0	9	2	1	0	13	3	8	0	1	3	0
RH	10	0	0	10	1	10	0	3	0	25	0	28	0	1	5	5
SM	4	1	0	21	0	21	1	11	0	36	0	42	4	2	3	4
U	2	0	0	0	0	0	0	0	11	0	2	0	3	0	2	17
V	4	1	4	0	18	0	0	17	1	11	0	0	0	15	0	55

+ uptrend, − downtrend

Blue: downtrends > 24%; red: uptrends > 24%

Table 5.

Meteorologically-dependent ozone by region (2010 emissions)

region:	NE	MA	MW	S	W	NW	WC	SW
ozone								
least conducive year	1994	1994	2002	1992	1993	1993	1993	2008
most conducive year	2000	1993	2009	2000	1998	1996	2003	2009

Table 6.

Temporal trends (ppb/year) in CMAQ ozone and emission-dependent ozone with a (95% confidence interval for the slope for different periods. Blue: significant negative slopes; red: significant positive slopes.

period:	**1990-2010**		**1990-2000**		**2000-2010**	
ozone:	**CMAQ**	**emission-dep**	**CMAQ**	**emission-dep**	**CMAQ**	**emission-dep**
Region						
NE	−0.39 (0.20)	−0.24 (0.02)	−0.25 (0.66)	−0.059(0.060)	−0.23 (0.63)	−0.65 (0.06)
MA	−0.62 (0.24)	−0.29 (0.03)	0.10 (0.64)	0.090 (0.06)	−0.83 (0.59)	−1.07 (0.20)
MW	−0.29 (0.26)	−0.18 (0.02)	−0.25 (0.66)	0.080(0.079)	−1.00 (0.71)	−0.69 (0.08)
S	−0.33 (0.28)	−0.19 (0.02)	0.62 (0.73)	0.15 (0.09)	−1.17 (0.76)	−0.75 (0.14)
W	0.11 (0.16)	−0.03 (0.01)	0.27 (0.42)	0.03 (0.05)	−0.40 (0.52)	−0.151(0.150)
NW	−0.01 (0.11)	−0.023 (0.004)	−0.09 (0.42)	0.001 (0.03)	0.00 (0.41)	−0.12 (0.02)
WC	0.005 (0.114)	−0.007 (0.001)	−0.05(0.32)	−0.025(0.029)	−0.01 (0.40)	−0.05 (0.02)
SW	−0.05 (0.19)	−0.07 (0.01)	0.40 (0.51)	0.024 (0.31)	−0.18 (0.10)	−0.25 (0.04)

Table 7.

Ozone variance attributed to meteorology and emissions

region:	NE	MA	MW	S	W	NW	WC	SW
met-dep. ozone by CMAQ meteorology (%)	98	96	95	85	77	91	91	96
emis-dep. ozone by emissions (%)	99	99	99	98	86	82	89	96
% total variability due to meteorology	36	19	55	54	39	86	90	92
% total variability due to emissions	51	74	46	52	33	9	1	19
% total due to meteorology and emissions	99	98	97	97	66	97	96	98
after detrending								
% total variability due to meteorology	88	51	85	82	34	95	94	97
% total variability due to emissions	8	34	43	43	59	11	2	39
% total due to meteorology and emissions	98	96	96	96	78	97	96	98

p = pressure, pb=boundary layer height, t = temperature, r = solar radiation, rh = relative humidity, u = u wind component, v = v wind component, ws = wind speed

Table 8.

Range of ozone response to emissions (ppb) source, 2000-2010, with 95% confidence intervals.

Region:	**NE**	**MA**	**MW**	**SE**	**W**	**NW**	**WC**	**SW**
emission								
ALL	6.4 ± 1.5	10.9 ± 1.1	6.8 ± 0.6	8.5 ± 0.5	2.5 ± 0.3	1.4 ± 0.8	1.4 ± 0.9	2.1 ± 0.6
NON-ROAD	0.7 ± 0.9	2.5 ± 0.9	1.3 ± 0.4	1.7 ± 0.4	0.5 ± 0.3	0.7 ± 0.7	0.1 ± 0.8	1.1 ± 0.4
NON-EGU POINT	0.9 ± 0.9	2.0 ± 0.9	1.1 ± 0.4	1.6 ± 0.4	0.3 ± 0.2	0.02 ± 0.5	0.2 ± 0.9	0.5 ± 0.4
EGU	0.4 ± 0.9	0.8 ± 0.7	0.5 ± 0.4	0.8 ± 0.3	0.04 ± 0.2	0.02 ± 0.5	0.3 ± 0.8	0.1 ± 0.3
AREA	1.8 ± 1.1	1.7 ± 0.8	0.9 ± 0.4	2.3 ± 0.4	2.1 ± 0.4	0.7 ± 0.6	0.4 ± 0.9	0.5 ± 0.4
MOBILE	2.9 ± 1.2	3.7 ± 0.9	2.3 ± 0.4	2.7 ± 0.4	0.6 ± 0.3	0.7 ± 0.6	0.1 ± 0.9	1.0 ± 0.4

Red indicates a confidence inter overlapping 0.